



## Original article

## Discovery of dihydroxylated 2,4-diphenyl-6-thiophen-2-yl-pyridine as a non-intercalative DNA-binding topoisomerase II-specific catalytic inhibitor



Kyu-Yeon Jun<sup>a</sup>, Hanbyeol Kwon<sup>a</sup>, So-Eun Park<sup>a</sup>, Eunyoung Lee<sup>a</sup>, Radha Karki<sup>b,1</sup>, Pritam Thapa<sup>b,1</sup>, Jun-Ho Lee<sup>c</sup>, Eung-Seok Lee<sup>b,\*</sup>, Youngjoo Kwon<sup>a,\*</sup>

<sup>a</sup> College of Pharmacy, Graduate School of Pharmaceutical Sciences, Ewha Global Top5, Ewha Womans University, Seoul 120-750, Republic of Korea

<sup>b</sup> College of Pharmacy, Yeungnam University, Gyeongsan 712-749, Republic of Korea

<sup>c</sup> Department of Emergency Medical Technology, Daejeon University, Daejeon 300-716, Republic of Korea

## ARTICLE INFO

## Article history:

Received 13 December 2013

Received in revised form

28 March 2014

Accepted 23 April 2014

Available online 24 April 2014

## Keywords:

Topoisomerase I

Topoisomerase II

Cytotoxicity

Anticancer agents

Dihydroxylated 2,4-diphenyl-6-thiophen-2-

yl-pyridines

3D-QSAR

## ABSTRACT

We describe our rationale for designing specific catalytic inhibitors of topoisomerase II (topo II) over topoisomerase I (topo I). Based on 3D-QSAR studies of previously published dihydroxylated 2,4-diphenyl-6-aryl pyridine derivatives, 9 novel dihydroxylated 2,4-diphenyl-6-thiophen-2-yl pyridine compounds were designed, synthesized, and their biological activities were evaluated. These compounds have 2-thienyl ring substituted on the R<sup>3</sup> group on the pyridine ring and they all showed excellent specificity toward topo II compared to topo I. *In vitro* experiments were performed for compound **13** to determine the mechanism of action for this series of compounds. Compound **13** inhibited topoisomerase II specifically by non-intercalative binding to DNA and did not stabilize enzyme-cleavable DNA complex. Compound **13** efficiently inhibited cell viability, cell migration, and induced G1 arrest. Also from 3D-QSAR studies, the results were compared with other previously published dihydroxylated 2,4-diphenyl-6-aryl pyridine derivatives to explain the structure–activity relationships.

© 2014 Elsevier Masson SAS. All rights reserved.

## 1. Introduction

DNA topoisomerases are enzymes that manipulate the topology of DNA. Topoisomerases are one of the most promising targets for development of anticancer agents because they are highly over-expressed in proliferating cancer cells [1]. Topoisomerases play an important role in various key cellular processes including replication, transcription, recombination, repair, and chromatin assembly [2,3]. There are two types of topoisomerases in humans, namely, topoisomerase type I (topo I) and type II (topo II). Topo I breaks and rejoins single-strand of a double helix while topo II breaks and rejoins double-strand DNA [4,5]. Because topo II breaks double-strand DNA, it can decatenate or catenate double-strand DNA rings that form during cell replication. The biological role of topo II is consistent with its expression pattern across the cell cycle,

whereby topo II $\alpha$ , among two subtypes of topo II, is primarily expressed in late S and G<sub>2</sub>-M phase cells [6].

$\alpha$ -Terpyridine is a heterocyclic compound derived from pyridine.  $\alpha$ -Terpyridine possesses three nitrogen atoms, and thus is able to form metal complexes [7] that bind to RNA/DNA [8,9]. We previously reported various terpyridine derivatives that possess topo I and II inhibitory activity and exhibit strong cytotoxicity against several human cancer cell lines [10–16]. Previous structure–activity relationship studies have shown that the 2-thienyl-4-furyl-pyridine skeleton has considerable topo I inhibitory activity [17]. Further, 2,6-dithienyl-4-furyl pyridine derivatives inhibit topo I and induce cytotoxicity, especially in the case of compounds having a methyl or chloride substitution on the thienyl and/or furyl ring [16]. A series of 2,4,6-triaryl pyridine derivatives containing chlorophenyl and phenolic moieties at the 2- and 4-position of the central pyridine were shown to inhibit both topo I and II [18]. Evaluation of these series of compounds indicated that when the 6-position of the central pyridine is substituted with a furyl, thienyl, or phenyl group instead of a pyridine group, specific inhibition of topo II is achieved. Furthermore, dihydroxylated 2,4,6-triphenyl pyridine derivatives exhibit stronger topo II inhibition compared

\* Corresponding author.

E-mail addresses: [eslee@ynu.ac.kr](mailto:eslee@ynu.ac.kr) (E.-S. Lee), [ykwon@ewha.ac.kr](mailto:ykwon@ewha.ac.kr) (Y. Kwon).

<sup>1</sup> Present address: Division of Hematology & Oncology, Department of Internal Medicine, Kansas University Medical Center, Kansas City, KS 66103, USA.

to topo I [19]. The position of the hydroxyl group appears to be important for these series of compounds, because hydroxyl groups at the *meta* or *para* position on either a 2- or 6-phenyl group result in cytotoxicity associated with specific inhibition of topo II. Despite these findings, a clear mechanism of action and mode of binding of these classes of compounds have not been established. While the skeletons of the terpyridine derivatives were very similar, the specificities for topo I and topo II varied widely. In this paper, dihydroxylated 2,4-diphenyl-6-thiophen-2-yl pyridine derivatives were evaluated for topo I and II inhibitory activity and cytotoxicity against several human cancer cell lines. *In vitro* experiments were performed to determine the mechanism of action for these series of compounds. In addition, we compared our 3D-QSAR results with those of previously published dihydroxylated 2,4-diphenyl-6-aryl pyridine derivatives to identify structure–activity relationships.

## 2. Chemistry

Dihydroxylated 2,4-diphenyl-6-thiophen-2-yl-pyridine derivatives **7–15** were synthesized in three steps as illustrated in Scheme 1. Using Claisen–Schmidt condensation reaction [20–23] nine dihydroxylated propenone intermediates were synthesized. Reactions were either base [20,21] or acid [22,23] catalyzed, without protection of hydroxyl groups. In the first method, 50% aqueous solution of KOH or 6 M NaOH was added to the solution of equimolar amounts of aryl ketone **1** ( $R^1 = a-c$ ) and aryl aldehyde **2** ( $R^2 = a-c$ ) in ethanol to obtain compounds **3–5** ( $R^1, R^2 = a-c$ ) in 36–90% yield. Another method utilized Lewis acid, borontrifluoro etherate ( $BF_3-Et_2O$ ). To a solution of aryl ketone **1** ( $R^1 = c$ ) and aryl aldehyde **2** ( $R^2 = c$ ) in dioxane was added  $BF_3-Et_2O$  to obtain compound **5** ( $R^1 = c, R^2 = c$ ) in 74% yield. In the second step, 2-thienyl pyridinium iodide salt **6** was synthesized in quantitative yield by the treatment of 2-acetyl thiophene with iodine in

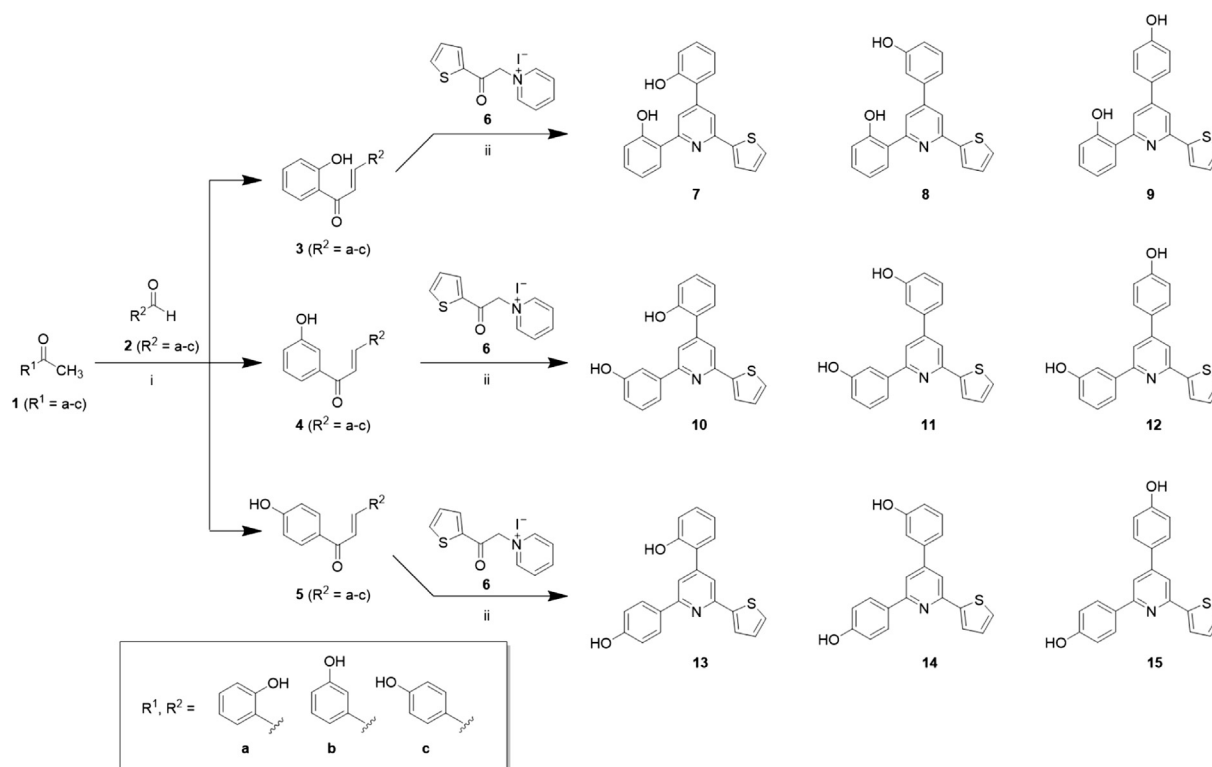
pyridine. Using modified Krohnke synthesis [24,25], final compounds **7–15** ( $R^1, R^2 = a-c$ ) were synthesized by the reaction of appropriate dihydroxylated chalcones **3–5** with pyridinium iodide salt **6** in the presence of ammonium acetate and glacial acetic acid (AcOH) in 49–92% yield.

The reaction gave a total of nine final compounds as shown in Scheme 1. All the compounds contain two hydroxyl moieties, one in each of the 2- and 4-phenyl ring of central pyridine. The hydroxyl moieties were substituted at various positions (*ortho*, *meta* or *para*) of the phenyl ring. Synthesis of dihydroxylated compounds allowed us to investigate the effect of the increase in the number of hydroxyl group on biological activity. Further, substitution of hydroxyl group at various positions (*ortho*, *meta* or *para*) of the phenyl ring helped us to evaluate the effect of hydroxyl position on biological activity.

## 3. Result and discussion

### 3.1. Evaluation of topoisomerase I and II inhibition

We synthesized nine dihydroxylated 2,4-diphenyl-6-thiophen-2-yl-pyridine compounds **7–15** that contained a hydroxyl group on each of the 2- and 4-phenyl rings in all possible positions (Scheme 1). The derivatives were then screened for their topo I and II inhibitory activities (Fig. S1 & Table 1). Topoisomerase inhibitory activities were determined by observation of relaxation of supercoiled pBR322 plasmid DNA. None of the synthesized compounds exhibited topo I inhibitory activity, because the supercoiled DNA (lower band marked SC) was transformed to a relaxed form (upper band marked Rel) by topo I with treatment of compounds (Fig. S1B). However, in the topo II relaxation assay, all of the compounds showed significant inhibitory effects at 100  $\mu$ M. Compounds **7–15** exhibited superior inhibition of topo II compared with the positive



**Scheme 1.** General synthetic scheme of dihydroxylated 2,4-diphenyl-6-thiophen-2-yl-pyridine derivatives. Reagents and conditions: (i) aryl aldehydes **2** ( $R^1 = a-c$ ) (1.0 equiv), KOH/NaOH/ $BF_3Et_2O$ , EtOH, 2–24 h, 20 °C, 36–90% yield; (ii)  $NH_4OAc$  (10.0 equiv), glacial AcOH, 12–24 h, 90–100 °C, 49–97% yield.

**Table 1**  
Topo II and I inhibitory activity and cytotoxicity of compounds 7–15.

Compounds	% Inhibition			IC <sub>50</sub> <sup>a</sup> (μM)				
	Topo II		Topo I	HCT15	K562	DU145	MCF-7	HeLa
	100 μM	20 μM	100 μM					
Etoposide	87.1	45.4		1.33 ± 0.10	2.09 ± 0.55	2.94 ± 0.04	3.25 ± 0.04	3.20 ± 0.57
Camptothecin			58.4	0.26 ± 0.04	1.18 ± 0.14	2.37 ± 0.55	3.91 ± 0.66	1.01 ± 0.01
Adriamycin				1.28 ± 0.07	2.85 ± 1.38	0.86 ± 0.04	3.69 ± 0.13	1.45 ± 0.01
<b>7</b>	97.5	40.1	0.0	4.32 ± 0.58	7.58 ± 0.47	35.30 ± 2.92	>50	16.06 ± 0.75
<b>8</b>	97.9	42.4	0.0	2.96 ± 0.09	1.52 ± 0.47	10.12 ± 0.19	>50	4.69 ± 0.54
<b>9</b>	96.8	18.1	0.0	2.66 ± 0.07	1.31 ± 0.15	>50	>50	>50
<b>10</b>	100	9.4	0.0	1.76 ± 0.35	3.62 ± 0.22	4.29 ± 0.04	12.01 ± 1.02	2.32 ± 0.25
<b>11</b>	100	24.3	1.0	1.12 ± 0.17	10.48 ± 2.35	2.70 ± 0.28	8.67 ± 0.10	15.98 ± 2.60
<b>12</b>	100	14.2	0.0	3.09 ± 0.02	1.80 ± 0.65	1.69 ± 0.18	5.72 ± 1.34	9.13 ± 1.61
<b>13</b>	98.0	37.3	0.0	0.84 ± 0.15	3.67 ± 0.10	3.12 ± 0.39	5.52 ± 0.13	1.87 ± 0.33
<b>14</b>	100	18.8	0.6	1.24 ± 0.14	4.12 ± 0.15	10.40 ± 0.46	2.70 ± 0.18	8.27 ± 1.24
<b>15</b>	100	19.4	5.4	0.73 ± 0.03	0.85 ± 0.04	1.53 ± 0.14	10.24 ± 0.24	2.08 ± 0.23

<sup>a</sup> Each data represents mean ± S.D. from three different experiments performed in triplicate.

control etoposide (Table 1). Furthermore, compounds **7**, **8**, and **13** had either greater or comparable inhibition at both 100 and 20 μM compared to etoposide. These results indicated that the dihydroxylated 2,4-diphenyl-6-thiophen-2-yl-pyridine compounds were specific to topo II, which was similar to previously reported results for dihydroxylated 2,4,6-triphenyl pyridines [19]. With respect to the dihydroxylated 2,4,6-triphenyl pyridines, the compounds with a hydroxyl group substituted at the 2- and 4-phenyl groups could be directly compared with **7**–**15** for the difference in properties between the phenyl group and thienyl group at the 6-position. Specifically, compounds with a 2-thienyl group exhibited superior topo II inhibition activity compared with compounds with a phenyl group on the 6-position of pyridine.

### 3.2. Cytotoxicity of the compounds

Five human cancer cell lines were used to evaluate the cytotoxicity of dihydroxylated 2,4-diphenyl-6-thiophen-2-yl-pyridine compounds: HCT15 (human colorectal adenocarcinoma cell line), K562 (human myeloid leukemic tumor cell line), DU145 (human prostate tumor cell line), MCF-7 (human breast adenocarcinoma cell line), and HeLa cells (human cervix tumor cell line). The inhibitory activities (IC<sub>50</sub>) of the tested compounds were expressed in micromolar concentration as illustrated in Table 1. Cells were treated with each compound for 48 h after which cytotoxicity was measured. The compounds were generally cytotoxic against most of the cell lines except for **9**, which was cytotoxic to HCT15 and K562 cells only. Among the tested compounds, **13** exhibited the highest and most uniform level of cytotoxicity, with an IC<sub>50</sub> value <6 μM for all of the cell lines tested. Based on these results, **13** was selected for further evaluation.

### 3.3. Compound **13** is topo II specific inhibitor

The results of screening the dihydroxylated 2,4-diphenyl-6-thiophen-2-yl-pyridine compounds indicated that they all inhibited topo II rather than topo I. Among the synthesized compounds, compound **13** exhibited the strongest potency for inhibition of topo II relaxation assay and produced the highest level of cytotoxicity. To further confirm the topo II inhibitory activity of compound **13**, we used a kinetoplast DNA (kDNA) decatenation assay. Through the specific catalytic activity of topo II, kDNA forms several decatenated forms of DNA including nicked (Nck), relaxed (Rel), and supercoiled (SC) DNA. Because of its size, catenated kDNA is unable to enter into agarose gels unless it is decatenated by topo II. Thus, the inhibitory activity of compound **13** was compared with the controls etoposide

and ellipticine at 100 μM (Fig. 1A). Etoposide does not affect the catalytic activity of topo II, since its cleavage step is reversible [26]. Conversely, treatment with ellipticine strongly inhibits topo II decatenation. These behaviors can be observed with gel electrophoresis, as decatenated products are the major product in samples treated with etoposide while the majority of kDNA remains in ellipticine treated samples (Fig. 1A). Compound **13** partially inhibited topo II decatenation at 50 μM, and fully inhibited topo II at 100 μM. This result indicated that compound **13** exhibited comparable or better efficacy than ellipticine. Together, these results confirmed that compound **13** is specific inhibitor of topo II.

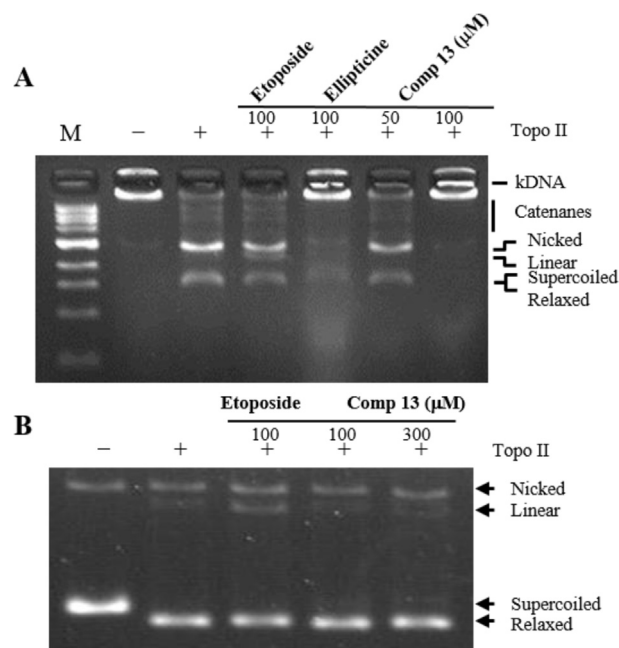


**Fig. 1.** Compound **13** is a topo II inhibitor. (A) kDNA decatenation assay with compound **13**. Topo II-mediated kDNA decatenation was inhibited by compound **13**. The positions of kDNA and other forms of DNA are indicated. (B) Cleavage complex assay. Three units of topo II were added to supercoiled pBR322 DNA 10 min before adding either etoposide or compound **13**. The formation of a linear band indicated that a cleavage complex was formed. As expected, treatment with etoposide formed a linear band, while compound **13** did not. Thus, compound **13** does not act as a topo II poison.

### 3.4. Compound **13** is catalytic inhibitor of topo II

The results of the kDNA decatenation assay showed that compound **13** is a topo II inhibitor. To further investigate the mechanism of action of compound **13**, we performed several in vitro experiments including unwinding, cleavage complex stabilization, and ATP competition assays. Topo II inhibitors can be categorized into two types, namely, topo II poisons and catalytic inhibitors [27]. Cleavage complex stabilization assays can be used to differentiate topo II poisons and catalytic inhibitors based on whether or not linear DNA is formed when topo II is added to supercoiled pBR322 DNA 10 min prior to addition of the test compound to initiate DNA relaxation. Electrophoresis can then be carried out in the presence of ethidium bromide to clearly visualize the linear form of DNA. Etoposide is a well-known topo II poison, and thus the linear form of DNA can be observed as a control (Fig. 1B). Conversely, treatment with compound **13** did not generate linear DNA at 100 and 300  $\mu\text{M}$ , and thus is not a topo II poison. Based on these data, compound **13** was deduced as a catalytic inhibitor of topo II.

### 3.5. Compound **13** does not intercalate into DNA

Topo II catalytic inhibitors can be classified as DNA intercalators and non-intercalators [28]. In topo II-catalyzed ATP hydrolysis and ATP competition assays, compound **13** exhibited neither inhibition of ATP hydrolysis nor any change in inhibition rate, indicating that it does not compete with ATP (data not shown) in the ATPase domain. Based on these results, compound **13** was next tested for its ability to intercalate into DNA. When DNA intercalators such as *m*-AMSA are briefly incubated with relaxed plasmid DNA, subsequent removal of the compound and enzyme results in re-supercoiling [29]. Thus, by using this assay, it is possible to differentiate between intercalators and non-intercalators. Negatively supercoiled DNA was first incubated with excess topo I to fully relax supercoiled DNA. Next, either compound **13** or *m*-AMSA, which was used as a positive control, was incubated with relaxed DNA and topo I. The results of this experiment indicated that compound **13** does not

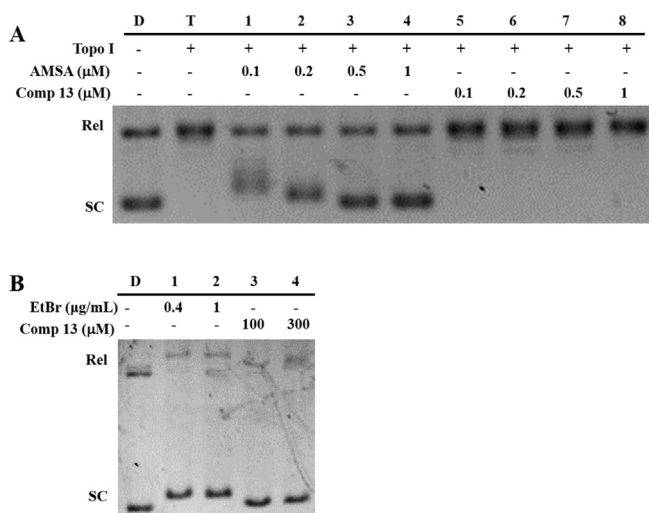


**Fig. 2.** Compound **13** is a topo II inhibitor. (A) Compound **13** does not intercalate into DNA as determined by a DNA unwinding assay. Lane D: pBR322 only; Lane T: pBR322 + Topo I; Lane 1–4: pBR322 + Topo I + *m*-AMSA in indicated concentrations; Lanes 5–8: pBR322 + Topo I + compound **13** at the indicated concentrations. (B) DNA intercalation assay. 1.25  $\mu\text{L}$  of negatively supercoiled DNA pBR322 (100 ng/ $\mu\text{L}$  Fermentas) and 100  $\mu\text{M}$  or 300  $\mu\text{M}$  of the test compound in a volume of 10  $\mu\text{L}$  was incubated at 37  $^{\circ}\text{C}$  for 20 min. Ethidium bromide at 0.4  $\mu\text{g/mL}$  and 1  $\mu\text{g/mL}$  were used as positive controls.

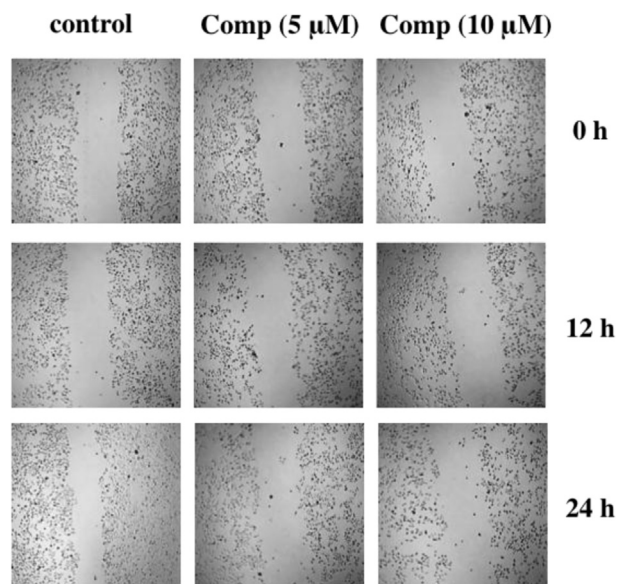


**Fig. 3.** Compound **13** inhibits the migration of HeLa cells. A clean wound was made in a 90% confluent monolayer of HeLa cells with a sterile micro tip. Cells were exposed to compound **13** at 5  $\mu\text{M}$  and 10  $\mu\text{M}$  for 24 h and were allowed to migrate in the medium.

intercalate with DNA (Fig. 2A). However, in a separate assay to measure intercalation by evaluating retardation of migration in gel electrophoresis, compound **13** was found to interact with DNA (Fig. 2B). Therefore, compound **13** was determined to inhibit topo II catalytically by binding to DNA in a non-intercalative mode.

### 3.6. Compound **13** induced apoptosis

Cell migration and proliferation can be easily evaluated by wound healing assay. HeLa cells were treated with various compounds at 5 or 10  $\mu\text{M}$  after making a wound. In untreated control cells, the gap wound narrowed over 24 h. However, in cells treated with compound **13**, the gap did not decrease after 24 h of treatment at 5  $\mu\text{M}$  (Fig. 3). For cells treated with compound **13** at 10  $\mu\text{M}$ , the edges of cells became rough and the gap width increased, indicating the presence of cell death. Thus, compound **13** inhibited cell migration in a dose-dependent manner, with higher doses resulting in apoptosis.

The mechanism of action of compound **13** was further investigated by observing its effects on cell cycle progression in HCT15 cells (Fig. 4A, B). Specifically, HCT15 cells were treated with compound **13** and cell cycle progression was analyzed by fluorescence activated cell sorting (FACS). The G0/G1 population increased as the concentration of compound **13** increased (0, 0.05, 0.1, 0.5, and 1  $\mu\text{M}$ ). In addition, a time dependent effect of the drug was observed after treating cells with 0.1  $\mu\text{M}$  of compound **13** at various time points (0, 4, 8, 12, and 24 h). This also increased the G0/G1 population as the time of treatment increased, reaching a maximum at 12 h. Therefore, compound **13** was determined to induce G0/G1 arrest in a both a time- and dose-dependent manner.

In order to determine whether the cytotoxic effects of compound **13** towards HCT15 cells were due to apoptosis, we next evaluated PARP cleavage, a marker of apoptosis, by western blot analysis (Fig. 4C). The amount of cleaved PARP increased as the concentration of drug treated increased (0, 0.5, 1, 2, and 4  $\mu\text{M}$ ), while increasing amounts of **13** had no effect on  $\alpha$ -tubulin expression, which was used as a loading control. Thus, our results indicated that compound **13** induced apoptosis in HCT15 cells in a dose dependent manner.

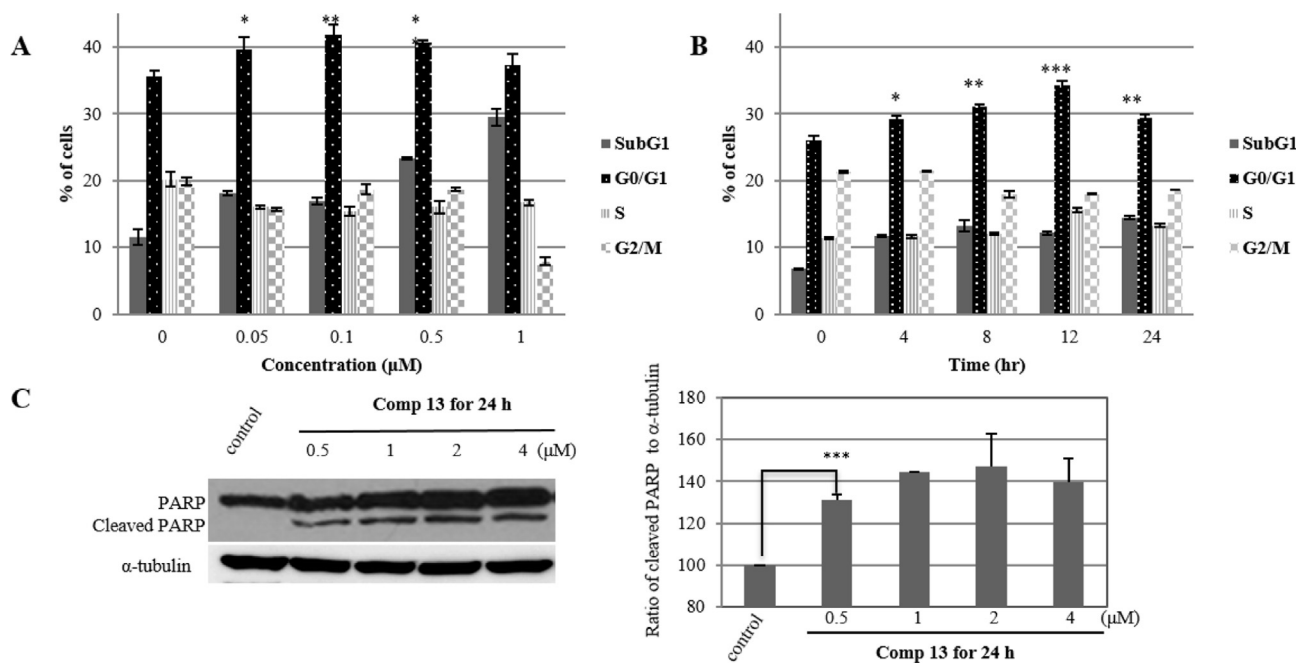


**Fig. 4.** Compound **13** induces apoptosis in HCT15 colon cancer cells. (A) Compound **13** induces G1 arrest in HCT15 colon cancer cells in a concentration dependent manner. Cell cycle distribution was evaluated by flow cytometric DNA content analysis. HCT15 cells were treated with **13** at 0.05, 0.1, 0.5 and 1 µM for 24 h (B) HCT15 cells were treated with **13** at 0.1 µM for various time points. (C) Western blot analysis of HCT15 whole cell lysates. Treatment of HCT15 cells with **13** resulted in increased PARP cleavage in a dose-dependent manner. The graph results and error bars show the mean  $\pm$  SD of triplicate experiments. \* $p < 0.05$  and \*\* $p < 0.01$ , and \*\*\* $p < 0.001$  compared with the vehicle control.

### 3.7. Analysis of the 3D structure–activity relationship

We next evaluated the structure activity relationships for the compounds synthesized in this study and those previously published, all of which shared a common pyridine core ring with substitutions at the 2, 4, and 6 positions [18,19]. The common structure for the 34 compounds used in the study was 2,4-diphenylpyridine ring and compound **13**, one of the most active inhibitors was selected as the template for alignment. Comparative molecular similarity index analysis (CoMSIA) can be used to quantify specific contributions of steric, electrostatic, hydrophobic,

and H-bonding factors that influence the cytotoxicity of small molecules [30,31]. According to CoMSIA, the cross-validated  $r^2$  ( $q^2$ ) of the training set was 0.709 with 2 components, while the non-cross-validated  $r^2$  was 0.842 with a standard error of estimate of 0.168. The donor and acceptor descriptors produced the most contributions (41.4% and 33.9%). Fig. 5 shows the contour maps for the H-bonding donor and acceptor fields based on the most active compound **13**. In the donor contour map (Fig. 5A), cyan represents regions that favor donor groups and purple the opposite. The H-bond donor groups were favored in *meta* and *para* site on R<sup>1</sup> and *ortho* and *meta* site on R<sup>2</sup> of the phenyl ring as it is represented as

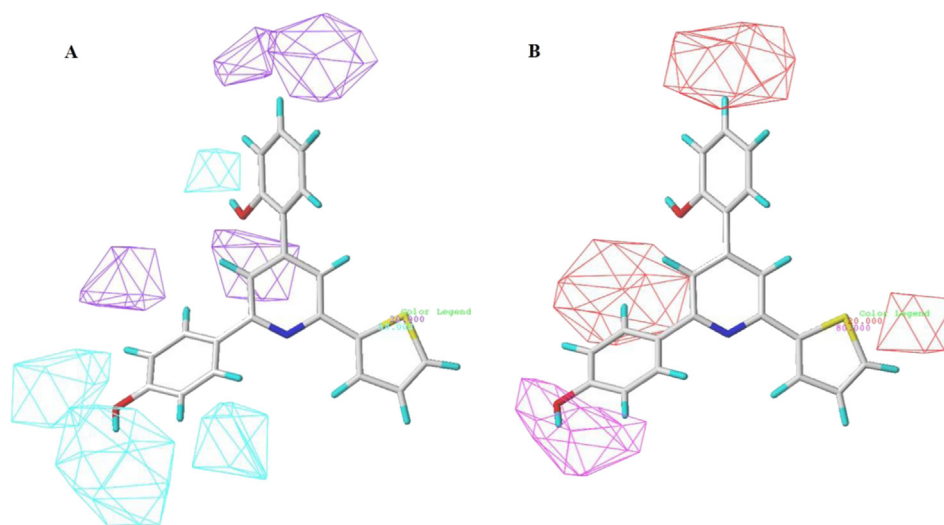


**Fig. 5.** CoMSIA contour maps of H-bond donor and acceptor fields based on compound **13**; (A) donor map. Cyan and purple indicate regions that favor and disfavor donor groups, respectively. (B) acceptor map. Magenta and red represents regions that favor and disfavor acceptor groups, respectively. (For interpretation of the references to colour in this figure legend, the reader is referred to the web version of this article.)

cyan contours. When the H-bond donors were in the *ortho* of R<sup>1</sup> and *para* of R<sup>2</sup>, the activity decreases as it is indicated by purple contours. Fig. 5B shows the acceptor field contour map where H-bond acceptor are favorable in magenta colored region and unfavorable in red. As it is indicated by magenta, the acceptor groups are favored in *meta* and *para* site on R<sup>1</sup>. When the acceptor groups are situated on the *ortho* of R<sup>1</sup> and *para* of R<sup>2</sup>, it is unfavorable according to the red contours. In addition, the red contour next to the R<sup>3</sup> aryl group represents that when acceptor atom is located on this region such as 3-pyridinyl group, it is unfavorable. The model was validated by a test set that included five compounds, indicated by asterisks in Table 2. The 3D-QSAR model gave good statistical results and good prediction using the test set. In summary, H-bonding was the most important factor for the activity of the compounds according to the CoMSIA model.

#### 4. Conclusions

In this study we designed, synthesized and tested 2,4-diphenyl-6-thiophen-2-yl-pyridine compounds for their ability to inhibit topoisomerases in an attempt to develop targeted anti-cancer drugs. The series of compounds showed excellent specificity towards topo II over topo I, and compound **13** was determined to be the most effective. Compound **13** was further analyzed to determine its mechanism of action, and was found to be a specific inhibitor of topo II through non-intercalative binding to DNA, and was able to inhibit cell viability and cell migration. We also performed a 3D-QSAR for the 2, 4, 6-aryl pyridine compounds. Based on five CoMSIA fields, H-bonding was found to be the highest contributing factor towards the cytotoxic effect of the compounds, with the position of the H-bond donor and acceptor being especially important. According to the contour plots, the H-bond donors and acceptors such as hydroxyl group was favored on the *meta* and *para* of R<sup>1</sup> and *ortho* of R<sup>2</sup> phenyl ring. The donor and acceptor groups on the *ortho* of R<sup>1</sup> and *para* of R<sup>2</sup> phenyl ring was unfavorable. Importantly, the insights gained from CoMSIA method provided valuable information that will be useful for designing new lead compounds exhibiting specificity towards topo II and anti-tumor activity.

#### 5. Experimental section

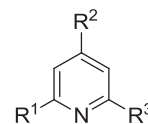
##### 5.1. Chemistry

Compounds used as starting materials and reagents were obtained from Aldrich and/or Junsei and were used without further purification. HPLC grade acetonitrile (ACN) and methanol were purchased from Burdick and Jackson, USA. Thin-layer chromatography (TLC) and column chromatography (CC) were performed using Kieselgel 60 F254 (Merck) and silica gel (Kieselgel 60, 230–400 mesh, Merck), respectively. Because all of the prepared compounds contained aromatic rings, they were visualized and detected on TLC plates by UV light (short wave, long wave or both). NMR spectra were recorded on a Bruker AMX 250 at 250 MHz (FT) for <sup>1</sup>H NMR and 62.5 MHz for <sup>13</sup>C NMR; chemical shifts were calibrated according to TMS. Chemical shifts ( $\delta$ ) and coupling constants (*J*) were recorded in ppm and hertz (Hz), respectively. Melting points were determined in open capillary tubes with an electrothermal 1A 9100 digital melting point apparatus and were uncorrected.

HPLC analyses were performed using two Shimadzu LC-10AT pumps gradient-controlled HPLC system equipped with a Shimadzu system controller (SCL-10A VP) and photo diode array detector (SPD-M10A VP) utilizing Shimadzu Class VP software. A sample volume of 10  $\mu$ L was injected into a Waters X-Terra<sup>®</sup> 5  $\mu$ M reverse-phase C<sub>18</sub> column (4.6  $\times$  250 mm) with a gradient elution

**Table 2**

Structures and biological activities of compounds used for CoMSIA.



No.	R <sup>1</sup>	R <sup>2</sup>	R <sup>3</sup>	Actual pIC <sub>50</sub>	CoMSIA predicted pIC <sub>50</sub>	CoMSIA residual
A1 <sup>a</sup>	2' OH phenyl	3 OH phenyl	2-furanyl	5.4101	5.1650	0.2448
A2	3' OH phenyl	3 OH phenyl	2-furanyl	5.6737	5.8251	-0.1514
A3	3' chlorophenyl	4 OH phenyl	2-furanyl	5.0958	5.1263	-0.0305
A4 <sup>a</sup>	3' chlorophenyl	3 OH phenyl	2-furanyl	5.6091	5.5269	0.0822
A5 <sup>a</sup>	4' chlorophenyl	3 OH phenyl	2-furanyl	4.9914	5.3800	-0.3886
B1	3' OH phenyl	2 OH phenyl	phenyl	6.0315	5.9563	0.0752
B2	3' OH phenyl	4 OH phenyl	phenyl	5.8996	5.7551	0.1445
B3	4' OH phenyl	2 OH phenyl	phenyl	6.0655	6.0226	0.0429
B4	4' OH phenyl	3 OH phenyl	phenyl	6.0555	6.0328	0.0227
B5	3' chlorophenyl	4 OH phenyl	phenyl	5.2147	5.2015	0.0131
B6	4' chlorophenyl	4 OH phenyl	phenyl	5.1599	5.2318	-0.0719
C1	3' OH phenyl	2 OH phenyl	2-pyridinyl	5.9706	5.9128	0.0578
C2 <sup>a</sup>	3' OH phenyl	3 OH phenyl	2-pyridinyl	5.8996	5.8970	0.0026
C3	2' OH phenyl	4 OH phenyl	3-pyridinyl	4.9739	4.9401	0.0338
C4	3' OH phenyl	4 OH phenyl	3-pyridinyl	5.5591	5.6434	-0.0843
C5	3' OH phenyl	2 OH phenyl	4-pyridinyl	5.7423	5.9670	-0.2247
C6	4' OH phenyl	2 OH phenyl	4-pyridinyl	5.983	6.0746	-0.0917
C7	4' OH phenyl	3 OH phenyl	4-pyridinyl	6.1427	6.0869	0.0557
C8	4' chlorophenyl	3 OH phenyl	4-pyridinyl	5.58	5.6134	-0.0334
8	2' OH phenyl	3 OH phenyl	2-thienyl	5.5287	5.4610	0.1191
10	3' OH phenyl	2 OH phenyl	2-thienyl	5.7545	5.8540	-0.0995
11	3' OH phenyl	3 OH phenyl	2-thienyl	5.9508	5.8649	0.0859
12	3' OH phenyl	4 OH phenyl	2-thienyl	5.51	5.6356	-0.1256
13	4' OH phenyl	2 OH phenyl	2-thienyl	6.0757	5.9597	0.1160
14	4' OH phenyl	3 OH phenyl	2-thienyl	5.9066	5.9707	-0.0641
D1	4' chlorophenyl	3 OH phenyl	2-thienyl	5.0325	5.3444	-0.3120
D2	4' chlorophenyl	4 OH phenyl	2-thienyl	5.1891	5.1155	0.0736
D3	2' OH phenyl	2 OH phenyl	3-thienyl	4.8652	5.1695	-0.3043
D4	2' OH phenyl	3 OH phenyl	3-thienyl	5.4908	5.1826	0.3081
D5	3' OH phenyl	2 OH phenyl	3-thienyl	6.0177	5.8483	0.1694
D6 <sup>a</sup>	3' OH phenyl	4 OH phenyl	3-thienyl	5.5528	5.6350	-0.0825
D7	4' OH phenyl	2 OH phenyl	3-thienyl	6.0706	5.9535	0.1171
D8	2' chlorophenyl	4 OH phenyl	3-thienyl	5.2343	5.1626	0.0717
D9	4' chlorophenyl	3 OH phenyl	3-thienyl	5.0531	5.3395	-0.2865

<sup>a</sup> Prediction set.

of 50%–100% of B in A for 15 min followed by 100%–50% of B in A for 15 min at a flow rate of 1.0 mL/min. UV detection was performed at 254 nm. The mobile phase A consisted of double distilled water with 20 mM ammonium formate (AF) and B was 90% ACN in water with 20 mM AF. Compound purities are described as percentages (%).

ESI LC/MS analyses were performed with a Finnigan LCQ Advantage<sup>®</sup> LC/MS/MS utilizing Xcalibur<sup>®</sup> software. For ESI LC/MS, LC was performed with an injection volume of 2  $\mu$ L on a Waters Atlantis<sup>®</sup> T3 reverse-phase C<sub>18</sub> column (2.1  $\times$  50 mm, 3  $\mu$ m). The mobile phase consisted of 100% distilled water (A) and 100% ACN with 20 mM AF (B). A gradient program was used at a flow rate of 200  $\mu$ L/min. The initial composition was 10% B and was programmed linearly to 90% B after 5 min and finally 10% B after 15 min. MS ionization conditions were as follows: Sheath gas flow rate, 70 arb; aux gas flow rate, 20 arb; I spray voltage, 4.5 kV; capillary temperature, 215  $^{\circ}$ C; column temperature, 40  $^{\circ}$ C; capillary voltage, 21 V; and tube lens offset, 10 V. Retention times are reported in minutes.

##### 5.1.1. General method for the preparation of **3**

Compound **3** was synthesized either by a KOH/NaOH or BF<sub>3</sub>–Et<sub>2</sub>O catalyzed Claisen–Schmidt condensation reactions.

KOH/NaOH catalyzed: To a solution of equimolar amounts of aryl ketone **1** ( $R^1 = a-c$ ) and aryl aldehyde **2** ( $R^1 = a-c$ ) in EtOH, a solution of either 50% aqueous KOH or 6 M NaOH was added and stirred for 2–24 h at 20 °C. The mixture was then neutralized with a solution of 6 M aqueous HCl (pH adjusted to 2). Lastly, the mixture was extracted with ethyl acetate, and washed with water and brine. Compound **3** was further purified by either recrystallization or column chromatography to yield pure solid compound.

$BF_3-Et_2O$  catalyzed: To a solution of aryl ketone **1** ( $R^1 = c$ ) and aryl aldehyde **2** ( $R^1 = c$ ) with minimal dioxane,  $BF_3-Et_2O$  was added gradually at 20 °C and stirred for 2 h. The mixture was then extracted with ethyl acetate and washed with water and brine. **3** was further purified by column chromatography to yield pure solid compound.

The synthesis of **3** ( $R^1, R^2 = a-c$ ) have been described previously [19].

### 5.1.2. General method for the preparation of **6**

Thiophen-2-yl ketone, iodine (1.2 equiv) and pyridine were refluxed at 140 °C for 3 h. A precipitate formed during the reaction, which was cooled to room temperature. The precipitate was then filtered and washed with cold pyridine to afford **6** in quantitative yield.

### 5.1.3. General method for the preparation of **7–15**

A mixture of the propenone intermediates **3–5** ( $R^1, R^2 = a-c$ ), pyridinium iodide salt **6**, and anhydrous ammonium acetate in glacial acetic acid was heated at 90–100 °C for 12–24 h. The reaction mixture was then extracted with ethyl acetate and washed with water and brine. The organic layer was dried with magnesium sulfate and filtered. The resulting filtrate was evaporated at reduced pressure and purified by silica gel column chromatography with gradient elution of ethyl acetate/*n*-hexane to afford solid compounds **7–15** in 49–92% yield. Nine dihydroxylated 2,4-diphenyl-6-thiophene-2-yl pyridine compounds were synthesized by this method.

### 5.1.4. Synthesis of 2,2'-[6-(Thiophen-2-yl)pyridine-2,4-diyl]diphenol (**7**)

Using the procedure described above, 1,3-bis(2-hydroxyphenyl)-propenone (345.96 mg, 1.44 mmol), dry ammonium acetate (1.10 g, 14.40 mmol), **6** (476.88 mg, 1.44 mmol) and AcOH (2 mL) were reacted to yield a yellow solid (248.00 mg, 49.9%, 0.71 mmol). mp = 223–224 °C,  $R_f$  (ethyl acetate/*n*-hexane 1:2 v/v) = 0.44, LC/MS/MS retention time = 8.90 min,  $[MH]^+$  = 346.22, and 97% purity by HPLC.  $^1H$  NMR (250 MHz, DMSO- $d_6$ )  $\delta$  13.56 (s, 1H, 2-phenyl 2-OH), 10.03 (br, 1H, 4-phenyl 2-OH), 8.19 (s, 1H, pyridine H-3), 8.09 (s, 1H, pyridine H-5), 8.07 (d,  $J = 7.3$  Hz, 1H, 2-phenyl H-6), 7.94 (dd,  $J = 3.6, 0.7$  Hz, 1H, 6-thiophene H-3), 7.76 (dd,  $J = 4.9, 0.7$  Hz, 1H, 6-thiophene H-5), 7.56 (dd,  $J = 7.5, 1.3$  Hz, 1H, 4-phenyl H-6), 7.36–7.27 (m, 2H, 2-phenyl H-4, 4-phenyl H-4), 7.24 (dd,  $J = 4.9, 3.8$  Hz, 1H, 6-thiophene H-4), 7.04–6.91 (m, 4H, 2-phenyl H-3, H-5, 4-phenyl H-3, H-5).  $^{13}C$  NMR (62.5 MHz, DMSO- $d_6$ )  $\delta$  158.86, 156.40, 155.10, 149.65, 149.04, 142.83, 131.68, 130.80, 130.73, 129.24, 128.92, 127.73, 126.75, 124.91, 119.91, 119.41, 119.00, 118.06, 117.89, 116.58.

### 5.1.5. Synthesis of 2-[4-(3-Hydroxyphenyl)-6-(thiophen-2-yl)pyridin-2-yl]phenol (**7**)

Using the procedure described above, 1-(2-hydroxyphenyl)-3-(3-hydroxyphenyl)propenone (360.37 mg, 1.50 mmol), dry ammonium acetate (1.15 g, 15.00 mmol), **6** (496.75 mg, 1.50 mmol), and AcOH (2 mL) were reacted to yield a yellow solid (449.60 mg, 86.8%, 1.30 mmol). mp = 224–225 °C,  $R_f$  (ethyl acetate/*n*-hexane 1:1 v/v) = 0.63, LC/MS/MS retention time = 8.71 min,

$[MH]^+$  = 346.22, and 100% purity by HPLC.  $^1H$  NMR (250 MHz, DMSO- $d_6$ )  $\delta$  13.47 (br, 1H, 2-phenyl 2-OH), 9.73 (br, 1H, 4-phenyl 3-OH), 8.24 (s, 1H, pyridine H-3), 8.21 (d,  $J = 8.9$  Hz, 1H, 2-phenyl H-6), 8.17 (s, 1H, pyridine H-5), 8.11 (dd,  $J = 3.8, 1.1$  Hz, 1H, 6-thiophene H-3), 7.77 (dd,  $J = 4.9, 1.0$  Hz, 1H, 6-thiophene H-5), 7.45 (t,  $J = 7.7$  Hz, 1H, 2-phenyl H-4), 7.40–7.31 (m, 3H, 4-phenyl H-5, H-6, H-2), 7.26 (dd,  $J = 4.9, 3.8$  Hz, 1H, 6-thiophene H-4), 6.98–6.92 (m, 3H, 4-phenyl H-4, 2-phenyl H-3, H-5).  $^{13}C$  NMR (62.5 MHz, DMSO- $d_6$ )  $\delta$  158.84, 158.20, 157.15, 150.83, 149.90, 142.70, 138.69, 131.76, 130.36, 129.21, 129.07, 128.09, 127.23, 119.38, 119.32, 118.42, 117.97, 116.84, 116.37, 115.17, 114.47.

### 5.1.6. Synthesis of 2-[4-(4-Hydroxyphenyl)-6-(thiophen-2-yl)pyridin-2-yl]phenol (**9**)

Using the procedure described above, 1-(2-hydroxyphenyl)-3-(4-hydroxyphenyl)propenone (264.27 mg, 1.10 mmol), dry ammonium acetate (847.88 mg, 11.00 mmol), **6** (364.28 mg, 1.10 mmol), and AcOH (2 mL) were reacted to yield a yellow solid (216.70 mg, 57.0%, 0.62 mmol). mp = 230–231 °C,  $R_f$  (ethyl acetate/*n*-hexane 1:1 v/v) = 0.58, LC/MS/MS retention time = 8.60 min,  $[MH]^+$  = 346.23, and 100% purity by HPLC.  $^1H$  NMR (250 MHz, DMSO- $d_6$ )  $\delta$  13.68 (s, 1H, 2-phenyl 2-OH), 9.94 (s, 1H, 4-phenyl 4-OH), 8.24 (s, 1H, pyridine H-3), 8.21 (m, 1H, 2-phenyl H-6), 8.17 (s, 1H, pyridine H-5), 8.09 (dd,  $J = 3.6, 1.3$  Hz, 1H, 6-thiophene H-3), 7.96 (d,  $J = 8.2$  Hz, 2H, 4-phenyl H-2, H-6), 7.76 (d,  $J = 5.0$  Hz, 1H, 6-thiophene H-5), 7.33 (t,  $J = 7.9$  Hz, 1H, 2-phenyl H-4), 7.25 (dd,  $J = 5.0, 3.9$  Hz, 1H, 6-thiophene H-4), 6.97 (d,  $J = 8.2$  Hz, 2H, 4-phenyl H-3, H-5), 6.95–6.92 (m, 2H, 2-phenyl H-3, H-5).  $^{13}C$  NMR (62.5 MHz, DMSO- $d_6$ )  $\delta$  159.53, 159.03, 157.15, 150.38, 149.72, 142.84, 131.74, 129.20, 129.18, 128.96, 128.00, 127.45, 127.13, 119.29, 119.26, 118.03, 116.11, 115.09, 114.18.

### 5.1.7. Synthesis of 2-[2-(3-Hydroxyphenyl)-6-(thiophen-2-yl)pyridin-4-yl]phenol (**10**)

Using the procedure described above, 3-(2-hydroxyphenyl)-1-(3-hydroxyphenyl)propenone (360.37 mg, 1.50 mmol), dry ammonium acetate (1.15 g, 15.00 mmol), **6** (496.75 mg, 1.50 mmol), and AcOH (2 mL) were reacted to yield a white solid (252.10 mg, 48.6%, 0.72 mmol). mp = 150–151 °C,  $R_f$  (ethyl acetate/*n*-hexane 1:1 v/v) = 0.56, LC/MS/MS retention time = 7.88 min,  $[MH]^+$  = 346.21, and 100% purity by HPLC.  $^1H$  NMR (250 MHz, DMSO- $d_6$ )  $\delta$  9.90 (br, 1H, 4-phenyl 2-OH), 9.61 (br, 1H, 2-phenyl 3-OH), 7.98 (s, 1H, pyridine H-3), 7.88 (s, 1H, pyridine H-5), 7.87 (dd,  $J = 3.5, 1.1$  Hz, 1H, 6-thiophene H-3), 7.66 (dd,  $J = 5.0, 0.8$  Hz, 1H, 6-thiophene H-5), 7.58 (t,  $J = 1.8$  Hz, 1H, 2-phenyl H-2), 7.55 (d,  $J = 7.4$  Hz, 1H, 2-phenyl H-6), 7.52 (dd,  $J = 7.3, 1.4$  Hz, 1H, 4-phenyl H-6), 7.30 (t,  $J = 7.8$  Hz, 1H, 2-phenyl H-5), 7.27 (td,  $J = 7.5, 1.5$  Hz, 1H, 4-phenyl H-4), 7.18 (dd,  $J = 4.9, 3.8$  Hz, 1H, 6-thiophene H-4), 7.02 (d,  $J = 8.2$  Hz, 1H, 4-phenyl H-3), 6.95 (t,  $J = 7.5$  Hz, 1H, 4-phenyl H-5), 6.86 (dd,  $J = 8.1, 1.7$  Hz, 1H, 2-phenyl H-4).  $^{13}C$  NMR (62.5 MHz, DMSO- $d_6$ )  $\delta$  157.98, 155.65, 155.03, 151.66, 148.41, 145.25, 140.09, 130.55, 130.39, 130.01, 128.65, 128.54, 125.50, 125.26, 119.85, 119.12, 117.60, 117.55, 116.54, 116.44, 113.67.

### 5.1.8. Synthesis of 3,3'-[6-(Thiophen-2-yl)pyridine-2,4-diyl]diphenol (**11**)

Using the procedure described above 1,3-bis(3-hydroxyphenyl)propenone (360.37 mg, 1.50 mmol), dry ammonium acetate (1.15 g, 15.00 mmol), **6** (496.75 mg, 1.50 mmol) and AcOH (2 mL) were reacted to yield a light yellow solid (443.50 mg, 85.6%, 1.28 mmol). mp = 114–115 °C,  $R_f$  (ethyl acetate/*n*-hexane 1:1 v/v) = 0.48, LC/MS/MS retention time = 7.69 min,  $[MH]^+$  = 346.21, and 100% purity by HPLC.  $^1H$  NMR (250 MHz, DMSO- $d_6$ )  $\delta$  9.63 (br, 2H, 2-phenyl 3-OH, 4-phenyl 3-OH), 8.07 (s, 1H, pyridine H-3), 8.02 (dd,  $J = 3.6, 0.9$  Hz, 1H, 6-thiophene H-3), 7.91 (s, 1H, pyridine H-5), 7.68 (dd,

$J = 5.3, 0.8$  Hz, 1H, 6-thiophene H-5), 7.65 (d,  $J = 1.9$  Hz, 1H, 2-phenyl H-2), 7.62 (d,  $J = 7.0$  Hz, 1H, 2-phenyl H-6), 7.37 (t,  $J = 7.8$  Hz, 1H, 2-phenyl H-5), 7.34–7.28 (m, 3H, 4-phenyl H-5, H-6, H-2), 7.20 (dd,  $J = 4.9, 3.7$  Hz, 1H, 6-thiophene H-4), 6.93–6.85 (m, 2H, 2-phenyl H-4, 4-phenyl H-4).  $^{13}\text{C}$  NMR (62.5 MHz, DMSO- $d_6$ )  $\delta$  158.23, 158.01, 156.51, 152.45, 149.86, 145.11, 139.88, 139.16, 130.42, 130.02, 128.86, 128.74, 126.07, 118.23, 117.82, 116.63, 116.54, 116.41, 115.02, 114.23, 113.84.

#### 5.1.9. Synthesis of 3-[4-(4-Hydroxyphenyl)-6-(thiophen-2-yl)pyridin-2-yl]phenol (**12**)

Using the procedure described above, 1-(3-hydroxyphenyl)-3-(4-hydroxyphenyl)propenone (360.37 mg, 1.50 mmol), dry ammonium acetate (1.15 g, 15.00 mmol), **6** (496.75 mg, 1.50 mmol), and AcOH (2 mL) were reacted to yield a white solid (433.60 mg, 83.7%, 1.25 mmol). mp = 249–250 °C,  $R_f$  (ethyl acetate/*n*-hexane 1:1 v/v) = 0.52, LC/MS/MS retention time = 7.55 min,  $[\text{MH}]^+ = 346.22$ , and 100% purity by HPLC.  $^1\text{H}$  NMR (250 MHz, DMSO- $d_6$ )  $\delta$  9.84 (br, 1H, 4-phenyl 4-OH), 9.59 (br, 1H, 2-phenyl 3-OH), 8.08 (s, 1H, pyridine H-3), 8.01 (dd,  $J = 3.8, 1.0$  Hz, 1H, 6-thiophene H-3), 7.93 (s, 1H, pyridine H-5), 7.88 (d,  $J = 8.6$  Hz, 2H, 4-phenyl H-2, H-6), 7.66 (dd,  $J = 4.7, 0.9$  Hz, 1H, 6-thiophene H-5), 7.64 (s, 1H, 2-phenyl H-2), 7.62 (d,  $J = 7.1$  Hz, 1H, 2-phenyl H-6), 7.31 (t,  $J = 8.1$  Hz, 1H, 2-phenyl H-5), 7.20 (dd,  $J = 4.9, 3.8$  Hz, 1H, 6-thiophene H-4), 6.94 (d,  $J = 8.6$  Hz, 2H, 4-phenyl H-3, H-5), 6.88 (dd,  $J = 7.2, 1.8$  Hz, 1H, 2-phenyl H-4).  $^{13}\text{C}$  NMR (62.5 MHz, DMSO- $d_6$ )  $\delta$  159.10, 157.95, 156.41, 152.32, 149.34, 145.34, 140.06, 129.92, 128.80, 128.64, 128.01, 125.82, 117.79, 116.48, 116.07, 115.49, 114.02, 113.84.

#### 5.1.10. Synthesis of 2-[2-(4-Hydroxyphenyl)-6-(thiophen-2-yl)pyridin-4-yl]phenol (**13**)

Using the procedures described in the SI, 3-(2-hydroxyphenyl)-1-(4-hydroxyphenyl)propenone (480.50 mg, 2.00 mmol), dry ammonium acetate (1.54 g, 20.00 mmol), **6** (662.34 mg, 2.00 mmol) and AcOH (2 mL) were reacted to yield a yellow solid (336.50 mg, 48.7%, 0.97 mmol) with a mp = 237–238 °C,  $R_f$  (ethyl acetate/*n*-hexane 1:1 v/v) = 0.51, LC/MS/MS retention time = 7.79 min,  $[\text{MH}]^+ = 346.21$ , and purity of 100% determined by HPLC.  $^1\text{H}$  NMR (250 MHz, DMSO- $d_6$ )  $\delta$  9.83 (br, 2H, 2-phenyl 4-OH, 4-phenyl 2-OH), 8.02 (d,  $J = 8.7$  Hz, 2H, 2-phenyl H-2, H-6), 7.90 (d,  $J = 0.8$  Hz, 1H, pyridine H-3), 7.85 (dd,  $J = 3.6, 0.8$  Hz, 1H, 6-thiophene H-3), 7.84 (d,  $J = 0.6$  Hz, 1H, pyridine H-5), 7.64 (dd,  $J = 5.0, 0.8$  Hz, 1H, 6-thiophene H-5), 7.50 (dd,  $J = 7.6, 1.5$  Hz, 1H, 4-phenyl H-6), 7.27 (td,  $J = 8.6, 1.6$  Hz, 1H, 4-phenyl H-4), 7.17 (dd,  $J = 5.0, 3.7$  Hz, 1H, 6-thiophene H-4), 7.02 (d,  $J = 8.2$  Hz, 1H, 4-phenyl H-3), 6.94 (t,  $J = 7.6$  Hz, 1H, 4-phenyl H-5), 6.91 (d,  $J = 8.7$  Hz, 2H, 2-phenyl H-3, H-5).  $^{13}\text{C}$  NMR (62.5 MHz, DMSO- $d_6$ )  $\delta$  158.77, 155.69, 154.88, 151.32, 148.22, 145.39, 130.38, 130.12, 129.55, 128.44, 128.14, 125.47, 125.10, 119.72, 117.88, 116.46, 115.66.

#### 5.1.11. Synthesis of 3-[2-(4-Hydroxyphenyl)-6-(thiophen-2-yl)pyridin-4-yl]phenol (**14**)

Using the procedure described above, 3-(3-hydroxyphenyl)-1-(4-hydroxyphenyl)propenone (360.37 mg, 1.50 mmol), dry ammonium acetate (1.15 g, 15.00 mmol), **6** (496.75 mg, 1.50 mmol), and AcOH (2 mL) were reacted to yield a white solid (475.70 mg, 91.8%, 1.37 mmol). mp = 212–213 °C,  $R_f$  (ethyl acetate/*n*-hexane 1:1 v/v) = 0.50, LC/MS/MS retention time = 7.63 min,  $[\text{MH}]^+ = 346.21$ , and 100% purity by HPLC.  $^1\text{H}$  NMR (250 MHz, DMSO- $d_6$ )  $\delta$  9.73 (br, 2H, 2-phenyl 4-OH, 4-phenyl 3-OH), 8.11 (d,  $J = 7.9$  Hz, 2H, 2-phenyl H-2, H-6), 8.00 (dd,  $J = 4.0, 0.9$  Hz, 1H, 6-thiophene H-3), 7.98 (s, 1H, pyridine H-3), 7.88 (s, 1H, pyridine H-5), 7.65 (dd,  $J = 5.0, 1.2$  Hz, 1H, 6-thiophene H-5), 7.36–7.33 (m, 2H, 4-phenyl H-5, H-6), 7.29 (s, 1H, 4-phenyl H-2), 7.19 (dd,  $J = 4.8, 3.8$  Hz, 1H, 6-thiophene H-4), 6.91

(d,  $J = 7.9$  Hz, 3H, 2-phenyl H-3, H-5, 4-phenyl H-4).  $^{13}\text{C}$  NMR (62.5 MHz, DMSO- $d_6$ )  $\delta$  159.05, 158.18, 156.52, 152.22, 149.73, 145.32, 139.35, 130.34, 129.35, 128.65, 128.47, 125.80, 118.17, 116.42, 115.73, 115.25, 114.20, 113.91.

#### 5.1.12. Synthesis of 4,4'-[6-(Thiophen-2-yl)pyridine-2,4-diyl]diphenol (**15**)

Using the procedure described above, 1,3-bis(4-hydroxyphenyl)propenone (240.25 mg, 1.00 mmol), dry ammonium acetate (770.80 mg, 10.00 mmol), **6** (331.17 mg, 1.00 mmol), and AcOH (2 mL) were reacted to yield a light yellow solid (258.40 mg, 74.8%, 0.74 mmol). mp = 229–230 °C,  $R_f$  (ethyl acetate/*n*-hexane 1:1 v/v) = 0.45, LC/MS/MS retention time = 7.48 min,  $[\text{MH}]^+ = 346.21$ , and 100% purity by HPLC.  $^1\text{H}$  NMR (250 MHz, DMSO- $d_6$ )  $\delta$  9.83 (br, 2H, 2-phenyl 4-OH, 4-phenyl 4-OH), 8.10 (d,  $J = 8.5$  Hz, 2H, 2-phenyl H-2, H-6), 7.99 (s, 1H, pyridine H-3), 7.97 (d,  $J = 3.6$  Hz, 1H, 6-thiophene H-3), 7.90 (s, 1H, pyridine H-5), 7.87 (d,  $J = 8.5$  Hz, 2H, 4-phenyl H-2, H-6), 7.64 (d,  $J = 4.9$  Hz, 1H, 6-thiophene H-5), 7.18 (t,  $J = 4.7$  Hz, 1H, 6-thiophene H-4), 6.93 (d,  $J = 8.2$  Hz, 2H, 2-phenyl H-3, H-5), 6.90 (d,  $J = 7.9$  Hz, 2H, 4-phenyl H-3, H-5).  $^{13}\text{C}$  NMR (62.5 MHz, DMSO- $d_6$ )  $\delta$  159.02, 158.95, 156.43, 152.15, 149.21, 145.57, 129.55, 128.76, 128.62, 128.47, 128.45, 128.21, 125.61, 116.05, 115.69, 114.32, 112.98.

### 5.2. Biological assays

#### 5.2.1. In vitro DNA topoisomerase I-mediated relaxation assay

A DNA topo I inhibition assay was performed as previously described by Fukuda et al. [32] with minor modifications. Briefly, compounds were dissolved in DMSO as 20 mM stock solutions. The activity of DNA topo I was determined by assessing the relaxation of supercoiled DNA pBR322. To this end, a mixture of 100 ng of plasmid pBR322 DNA and 1 unit of recombinant human DNA topo I (TopoGEN INC., USA) was incubated with or without the as-prepared compounds at 37 °C for 30 min in relaxation buffer (10 mM Tris–HCl (pH 7.9), 150 mM NaCl, 0.1% bovine serum albumin, 1 mM spermidine, and 5% glycerol). The reaction was terminated by adding 2.5  $\mu\text{L}$  of a stop solution (5% sarcosyl, 0.0025% bromophenol blue and 25% glycerol) to a final volume of 10  $\mu\text{L}$ . DNA samples were then electrophoresed on a 1% agarose gel at 50 V for 1 h in Tris–acetate–EDTA (TAE) running buffer. Gels were stained for 30 min in an aqueous solution of ethidium bromide (0.5  $\mu\text{g}/\text{mL}$ ). DNA bands were visualized by UV-transillumination and quantitated using Alphamager™ software (Alpha Innotech Corporation).

#### 5.2.2. In vitro DNA topoisomerase II-mediated inhibition assay

The DNA topo II inhibitory activity of compounds were measured as follows [33]. A mixture of 200 ng of supercoiled pBR322 plasmid DNA and 1 unit of human DNA topoisomerase II $\alpha$  (USB, USA) was incubated with or without the as-prepared compounds in assay buffer (10 mM Tris–HCl (pH 7.9) containing 50 mM NaCl, 5 mM MgCl<sub>2</sub>, 1 mM EDTA, 1 mM ATP, and 15  $\mu\text{g}/\text{mL}$  bovine serum albumin) for 30 min at 30 °C. The reaction was terminated by the addition of 3  $\mu\text{L}$  of 7 mM EDTA to a final volume of 20  $\mu\text{L}$ . Reaction products were analyzed on a 1% agarose gel running at 50 V for 1 h in TAE buffer. Gels were stained for 30 min in an aqueous solution of ethidium bromide (0.5  $\mu\text{g}/\text{mL}$ ). DNA bands were visualized by UV-transillumination and supercoiled DNA was quantitated using Alphamager™ software (Alpha Innotech Corporation).

#### 5.2.3. Cytotoxicity assay

Cancer cells were cultured according to the supplier's instructions. For the cytotoxicity assay, cells were seeded in 96-well plates at a density of 2–4  $\times 10^4$  cells per well and incubated overnight in 0.1 mL of media supplemented with 10% Fetal Bovine

Serum (Hyclone, USA) in an incubator at 37 °C with a 5% CO<sub>2</sub> atmosphere. The following day the culture medium in each well was exchanged with 0.1 mL aliquots of medium containing varying concentrations of compounds. On the fourth day, 5 µL of cell counting kit-8 solution (Dojindo, Japan) was added to each well, and plates were incubated for an additional 4 h under the same conditions [34]. The absorbance of each well was then determined with an Automatic Elisa Reader System (Bio-Rad 3550) at a wavelength of 450 nm. To determine IC<sub>50</sub> values, absorbance readings at 450 nm were fitted to a four-parameter logistic equation. Adriamycin, etoposide, and camptothecin were purchased from Sigma and used as positive controls.

#### 5.2.4. kDNA decatenation assay

Topo II specificity was determined using a kDNA decatenation assay [35]. Briefly, the assay was performed in a total reaction volume of 10 µL containing 50 mM Tris–HCl (pH 8.0), 120 mM KCl, 10 mM MgCl<sub>2</sub>, 0.5 mM dithiothreitol, 0.5 mM ATP, 30 µg/mL bovine serum albumin, and 75 ng of kDNA. Compounds were added to a final concentration of 50, 100 µM in 1% DMSO. Reactions were initiated by addition of 2–4 units of topo II, followed by incubation with the compound mixtures for 30 min at 37 °C. Reactions were terminated by the addition of 2.5 µL of stop solution (5% SDS, 25% ficoll, and 0.05% bromophenol blue) followed by treatment with 0.25 mg/mL proteinase K (Roche) at 55 °C for 30 min to eliminate protein. Samples were resolved by electrophoresis on a 1.2% (w/v) agarose gel containing 0.5 µg/mL ethidium bromide in TAE buffer (100 mM Tris–acetate and 2 mM Na<sub>2</sub>EDTA, pH 8.3). DNA bands were visualized by UV and photographed and documented with AlphaMager™ software (Alpha Innotech Corporation). For quantitation of the substrate (kDNA) and products of the topo II reaction (Nck, SC, and catenanes), the numerical values of intensity profiles of the different lanes were obtained after background subtraction and exported to Microsoft Excel. For each lane, the overall intensity was used to obtain the fraction of the intensity for the different bands, namely, kDNA, Nck, and SC. We subsequently determined topo II activity based on the relative amounts of the final products (nicked plus supercoiled minicircles). A positive control (1% DMSO, topo II) and negative control (1% DMSO) were used to establish limit values (1 and 0, respectively).

#### 5.2.5. Cleavage complex stabilization assay

For the cleavage complex assay, supercoiled DNA pBR322 (Fermentas) was used as a substrate, and 3 units of topo II (TopoGEN, USA) were added 10 min before the addition of test compounds. The reaction mixture was incubated at 37 °C for 20 min and the reaction was stopped by addition of 10% SDS followed by digestion with proteinase K at 45 °C for 30 min. After addition of loading buffer, the reaction mixture was heated for 2 min at 70 °C. Finally, electrophoresis was carried out with a 0.8% agarose gel in TAE buffer containing 0.5 µg/mL ethidium bromide, followed by destaining the gel with water for 20 min.

#### 5.2.6. DNA unwinding assay

The DNA-unwinding capacity of compound **13** was analyzed using a DNA unwinding kit (TopoGEN, Port Orange, FL, USA) according to the manufacturer's instructions. Briefly, 100 ng plasmid (pHOT1) was treated with 2 U of topo I (TopoGEN, Port Orange, FL, USA) in 20 µL of buffer (10 mM Tris–HCl, pH 7.5, 1 mM EDTA) for 30 min at 37 °C. Relaxed plasmids were then incubated in the presence of various test compounds at 37 °C for an additional 30 min *m*-AMSA (100, 200, 500, and 1000 µM) was used as a positive control for DNA unwinding activity. At the end of the incubation, 1% SDS and loading dye were added to terminate the reactions. The resulting aqueous phase was resolved on 1% agarose

gels at 15 V/cm for 12–15 h. After electrophoresis, gels were stained in TAE buffer with ethidium bromide for 30 min and visualized using an Alpha Tech Imager.

In a separate assay, we determined inhibition of DNA unwinding activity as retardation of migration of DNA [36]. Briefly, 1.25 µL of negatively supercoiled DNA pBR322 (100 ng/µL Fermentas) and 100 µM or 300 µM of investigational compounds in a total volume of 10 µL was incubated at 37 °C for 20 min. Positive controls consisted of 0.4 µg/mL and 1 µg/mL ethidium bromide. Next, mixtures were resolved on 1% agarose gels at 20 vol/cm for 12–16 h. After electrophoresis, gels were stained in 1× TAE buffer with ethidium bromide for 30 min and visualized using an Alpha Tech Imager.

#### 5.2.7. Cell cycle analysis

HCT15 cells were seeded in 60 mm dishes at a density of  $5 \times 10^5$  cells per dish. When cells reached 80% confluency, they were treated with the test compounds at concentrations of 0.05, 0.1, 0.5, and 1 µM. Cells were then washed with ice-cold PBS (pH 7.4) and harvested by centrifugation at 2000 rpm for 5 min. The resulting pellets were fixed with 70% ethanol, and fixed cells were then washed with PBS before incubation with 50 µg/mL propidium iodide (Sigma, USA) and 2.5 µg/mL RNase (Sigma, USA). Fluorescence was measured with a Fluorescence-Activated Cell Sorting (FACS)-Caliber flow cytometer (BD Biosciences, USA). At least 10,000 cells were measured for each sample [37].

#### 5.2.8. Wound healing assay

HeLa cells were cultured in 6-well plates to 90% confluency. A clean wound in the cell monolayer then created across the center of the well with a sterile micro tip. After starvation with low serum media (1% FBS in DMEM) for 4 h, cells were exposed to the compound at either 5 or 10 µM and allowed to migrate in the medium. The wound was assessed by microscopy at 5× magnification at different time points (0, 12 and 24 h).

#### 5.2.9. Western blot assay

HCT15 cells were grown on 60 mm tissue culture dishes at  $1 \times 10^6$  cells until reaching 80% confluency. The cells were then treated with compound **13** at various concentrations (0, 0.5, 1, 2, 4 µM) for 24 h. Cells were lysed in lysis buffer solution containing 50 mM Tris–HCl, 300 mM NaCl, 1% Triton X-100, 10% glycerol, 1.5 mM MgCl<sub>2</sub>, 1 mM CaCl<sub>2</sub>, 1 mM PMSF, and 1% protease inhibitor cocktail. Protein concentrations of soluble extracts of lysates were then determined by BCA™ Protein Assay Kit (Pierce, USA) and a total of 60 µg protein per sample was loaded on a 12% polyacrylamide gel, which was then transferred to a polyvinylidene fluoride membrane (Millipore Corporation, USA). Next, membranes were blocked for 1 h at room temperature in TBST with 5% skim milk. Membranes were incubated with antibodies for either of  $\alpha$ -tubulin or PARP (1:1000) in TBST with 5% skim milk overnight at 4 °C. Anti-rabbit IgG horseradish peroxidase was used as the secondary antibody. After incubation antibodies, membranes were washed three times with TBST and detected with ECL plus western blotting detection reagent (Ab Frontier, Korea). Western blot images were analyzed using Multi-Gauge Software (Fuji Photo Film Co., Ltd., Japan).

#### 5.2.10. Statistical analysis

Data were expressed as the mean  $\pm$  standard deviation (SD), with at least 3 replicates per experimental group. Comparison of differences was conducted using unpaired, two-tailed Student *t*-test. Differences with *p* values  $\leq 0.05$  were considered statistically significant.

### 5.3. Computational analysis

The datasets generated in this study as well as those curated from published studies comprised 34 compounds. The structures of compounds and their biological data are shown in Table 2. In order to analyze the structure activity relationships, we used the common biological data, which consisted of the IC<sub>50</sub> values for the HCT15 cell line. IC<sub>50</sub> values in units of molarity (M) were transformed to negative log values. The 3D compound structures were prepared using Sybyl X-2.0 [38]. The lowest energy Gasteiger–Hückel charges were applied to each molecule and energy minimization was performed using the Tripos force field. Compound **13** was used as a template and the remaining compounds were manually aligned using the common core ring structure. The torsion angles the 2, 4, and 6-aryl groups were adjusted to match those of compound **13**. When adjusting the torsion angles, all the possible combinations of rotational conformations were checked to find the lowest energy conformer and each compounds were energetically minimized using the same method as above. The final alignment of 3D-QSAR data for compounds was analyzed using the CoMSIA descriptors. The CoMSIA model generated using the pIC<sub>50</sub> data from HCT15 cells was validated by predicting a test set consisting of 5 compounds.

### Acknowledgments

This research was supported by the Basic Science Research Program through the National Research Foundation of Korea (NRF) funded by the Ministry of Education, Science and Technology (2011–0011007). K.-Y. Jun was supported by RP-Grant 2012 of Ewha Womans University.

### Abbreviations

Topo	topoisomerase
kDNA	kinetoplast DNA
Nck	nicked
Rel	relaxed
SC	supercoiled
ACN	acetonitrile
TLC	thin-layer chromatography
CC	column chromatography
AF	ammonium formate
DMSO	dimethylsulfoxide
TAE	Tris–acetate–EDTA
IC <sub>50</sub>	50% inhibitory concentration
SDS	sodium dodecyl sulfate
SD	standard deviation.

### Appendix A. Supplementary data

Supplementary data related to this article can be found at <http://dx.doi.org/10.1016/j.ejmech.2014.04.066>.

### References

- [1] M.M. Heck, W.C. Earnshaw, Topoisomerase II: a specific marker for cell proliferation, *The Journal of Cell Biology* 103 (1986) 2569–2581.
- [2] J.B. Leppard, J.J. Champoux, Human DNA topoisomerase I: relaxation, roles, and damage control, *Chromosoma* 114 (2005) 75–85.
- [3] S.M. Vos, E.M. Tretter, B.H. Schmidt, J.M. Berger, All tangled up: how cells direct, manage and exploit topoisomerase function, *Nature reviews. Molecular Cell Biology* 12 (2011) 827–841.
- [4] J.J. Champoux, DNA topoisomerases: structure, function, and mechanism, *Annual Review of Biochemistry* 70 (2001) 369–413.
- [5] J.C. Wang, Moving one DNA double helix through another by a type II DNA topoisomerase: the story of a simple molecular machine, *Quarterly Reviews of Biophysics* 31 (1998) 107–144.
- [6] R.D. Woessner, M.R. Mattern, C.K. Mirabelli, R.K. Johnson, F.H. Drake, Proliferation- and cell cycle-dependent differences in expression of the 170 kilodalton and 180 kilodalton forms of topoisomerase II in NIH-3T3 cells, *Cell Growth & Differentiation* 2 (1992) 209–214.
- [7] G. Lowe, A.-S. Droz, J.J. Park, G.W. Weaver, The design and synthesis of bis-[4'-azido-2,2':6',2''-terpyridine platinum(II)] complexes with rigid and extended linkers for studying the topology of DNA by photoaffinity labeling, *Bioorganic Chemistry* 27 (1999) 477–486.
- [8] Y.C. Lo, T.P. Ko, W.C. Su, T.L. Su, A.H. Wang, Terpyridine-platinum(II) complexes are effective inhibitors of mammalian topoisomerases and human thioredoxin reductase 1, *Journal of Inorganic Biochemistry* 103 (2009) 1082–1092.
- [9] P.J. Carter, C.C. Cheng, H.H. Thorp, Oxidation of DNA and RNA by oxoruthenium(IV) metallointercalators: visualizing the recognition properties of dipyrrophenazine by high-resolution electrophoresis, *Journal of the American Chemical Society* 120 (1998) 632–642.
- [10] L.X. Zhao, T.S. Kim, S.H. Ahn, T.H. Kim, E.K. Kim, W.J. Cho, H. Choi, C.S. Lee, J.A. Kim, T.C. Jeong, C.J. Chang, E.S. Lee, Synthesis, topoisomerase I inhibition and antitumor cytotoxicity of 2,2':6',2''-, 2,2':6',3''- and 2,2':6',4''-terpyridine derivatives, *Bioorganic & Medicinal Chemistry Letters* 11 (2001) 2659–2662.
- [11] L.X. Zhao, J. Sherchan, J.K. Park, Y. Jahng, B.S. Jeong, T.C. Jeong, C.S. Lee, E.S. Lee, Synthesis, cytotoxicity and structure-activity relationship study of terpyridines, *Archives of Pharmacological Research* 29 (2006) 1091–1095.
- [12] A. Basnet, P. Thapa, R. Karki, Y. Na, Y. Jahng, B.S. Jeong, T.C. Jeong, C.S. Lee, E.S. Lee, 2,4,6-Trisubstituted pyridines: synthesis, topoisomerase I and II inhibitory activity, cytotoxicity, and structure-activity relationship, *Bioorganic & Medicinal Chemistry* 15 (2007) 4351–4359.
- [13] J.K. Son, L.X. Zhao, A. Basnet, P. Thapa, R. Karki, Y. Na, Y. Jahng, T.C. Jeong, B.S. Jeong, C.S. Lee, E.S. Lee, Synthesis of 2,6-diaryl-substituted pyridines and their antitumor activities, *European Journal of Medicinal Chemistry* 43 (2008) 675–682.
- [14] P. Thapa, R. Karki, A. Basnet, U. Thapa, H. Choi, Y. Na, Y. Jahng, C.-S. Lee, Y. Kwon, B.-S. Jeong, E.-S. Lee, 2,6-Dithienyl-4-arylpyridines: synthesis, topoisomerase I and II inhibition and structure-activity relationship, *Bulletin of the Korean Chemical Society* 29 (2008) 1605–1608.
- [15] P. Thapa, R. Karki, U. Thapa, Y. Jahng, M.J. Jung, J.M. Nam, Y. Na, Y. Kwon, E. Lee, S. 2-Thienyl-4-furyl-6-aryl pyridine derivatives: synthesis, topoisomerase I and II inhibitory activity, cytotoxicity, and structure-activity relationship study, *Bioorganic & Medicinal Chemistry* 18 (2010) 377–386.
- [16] A. Basnet, P. Thapa, R. Karki, H. Choi, J.H. Choi, M. Yun, B.S. Jeong, Y. Jahng, Y. Na, W.J. Cho, Y. Kwon, C.S. Lee, E.S. Lee, 2,6-Dithienyl-4-furyl pyridines: synthesis, topoisomerase I and II inhibition, cytotoxicity, structure-activity relationship, and docking study, *Bioorganic & Medicinal Chemistry Letters* 20 (2010) 42–47.
- [17] L.X. Zhao, Y.S. Moon, A. Basnet, E.K. Kim, Y. Jahng, J.G. Park, T.C. Jeong, W.J. Cho, S.U. Choi, C.O. Lee, S.Y. Lee, C.S. Lee, E.S. Lee, Synthesis, topoisomerase I inhibition and structure-activity relationship study of 2,4,6-trisubstituted pyridine derivatives, *Bioorganic & Medicinal Chemistry Letters* 14 (2004) 1333–1337.
- [18] P. Thapa, R. Karki, M. Yun, T.M. Kadayat, E. Lee, H.B. Kwon, Y. Na, W.J. Cho, N.D. Kim, B.S. Jeong, Y. Kwon, E.S. Lee, Design, synthesis, and antitumor evaluation of 2,4,6-triaryl pyridines containing chlorophenyl and phenolic moiety, *European Journal of Medicinal Chemistry* 52 (2012) 123–136.
- [19] R. Karki, P. Thapa, H.Y. Yoo, T.M. Kadayat, P.H. Park, Y. Na, E. Lee, K.H. Jeon, W.J. Cho, H. Choi, Y. Kwon, E.S. Lee, Dihydroxylated 2,4,6-triphenyl pyridines: synthesis, topoisomerase I and II inhibitory activity, cytotoxicity, and structure-activity relationship study, *European Journal of Medicinal Chemistry* 49 (2012) 219–228.
- [20] Y. Jahng, L.X. Zhao, Y.S. Moon, A. Basnet, E.K. Kim, H.W. Chang, H.K. Ju, T.C. Jeong, E.S. Lee, Simple aromatic compounds containing propenone moiety show considerable dual COX/5-LOX inhibitory activities, *Bioorganic & Medicinal Chemistry Letters* 14 (2004) 2559–2562.
- [21] D. Batovska, S. Parushev, A. Slavova, V. Bankova, I. Tsvetkova, M. Ninova, H. Najdenski, Study on the substituents' effects of a series of synthetic chalcones against the yeast *Candida albicans*, *European Journal of Medicinal Chemistry* 42 (2007) 87–92.
- [22] D.S. Breslow, C.R. Hauser, Condensations. XI. Condensations of certain active hydrogen compounds effected by borontrifluoride and aluminum chloride, *Journal of the American Chemical Society* 62 (1940) 2385–2388.
- [23] T. Narendar, K.P. Reddy, A simple and highly efficient method for the synthesis of chalcones by using borontrifluoride-etherate, *Tetrahedron Letters* 48 (2007) 3177–3180.
- [24] F. Kröhnke, The specific synthesis of pyridines and oligopyridines, *Synthesis* 1976 (1976) 1–24.
- [25] F. Kröhnke, Synthesis using pyridinium salts (IV), *Angewandte Chemie* 2 (1963) 380–393.
- [26] N. Osheroff, Effect of antineoplastic agents on the DNA cleavage/religation reaction of eukaryotic topoisomerase II: inhibition of DNA religation by etoposide, *Biochemistry* 28 (1989) 6157–6160.
- [27] C. Bailly, Contemporary challenges in the design of topoisomerase II inhibitors for cancer chemotherapy, *Chemical Reviews* 112 (2012) 3611–3640.
- [28] J.M. Besterman, L.P. Elwell, E.J. Cragoe Jr., C.W. Andrews, M. Cory, DNA intercalation and inhibition of topoisomerase II. Structure-activity

- relationships for a series of amiloride analogs, *The Journal of Biological Chemistry* 264 (1989) 2324–2330.
- [29] Y. Pommier, J.M. Covey, D. Kerrigan, J. Markovits, R. Pham, DNA unwinding and inhibition of mouse leukemia L1210 DNA topoisomerase I by intercalators, *Nucleic Acids Research* 15 (1987) 6713–6731.
- [30] G. Klebe, U. Abraham, T. Mietzner, Molecular similarity indices in a comparative analysis (CoMSIA) of drug molecules to correlate and predict their biological activity, *Journal of Medicinal Chemistry* 37 (1994) 4130–4146.
- [31] G. Klebe, U. Abraham, Comparative molecular similarity index analysis (CoMSIA) to study hydrogen-bonding properties and to score combinatorial libraries, *Journal of Computer-aided Molecular Design* 13 (1999) 1–10.
- [32] M. Fukuda, K. Nishio, F. Kanzawa, H. Ogasawara, T. Ishida, H. Arioka, K. Bonjanowski, M. Oka, N. Saijo, Synergism between cisplatin and topoisomerase I inhibitors, NB-506 and SN-38, in human small cell lung cancer cells, *Cancer Research* 56 (1996) 789–793.
- [33] D.H. Kang, J.S. Kim, M.J. Jung, E.-S. Lee, Y. Jhang, Y. Kwon, Y. Na, New insight for fluoroquinophenoxazine derivatives as possibly new potent topoisomerase I inhibitor, *Bioorganic & Medicinal Chemistry Letters* 18 (2008) 1520–1524.
- [34] S.H. Park, S.J. Park, J.O. Kim, J.H. Shin, E.S. Kim, Y.K. Jo, J.S. Kim, S.J. Park, D.H. Jin, J.J. Hwang, S.J. Lee, S.Y. Jeong, C. Lee, I. Kim, D.H. Cho, Down-regulation of survivin by nemadipine-A sensitizes cancer cells to TRAIL-induced apoptosis, *Biomolecules and Therapeutics* 21 (2013) 29–34.
- [35] K. Tanabe, Y. Ikegami, R. Ishida, T. Andoh, Inhibition of topoisomerase II by antitumor agents bis(2,6-dioxopiperazine) derivatives, *Cancer Research* 51 (1991) 4903–4908.
- [36] A.T. Bavisar, C. Madaan, R. Preet, P. Mohapatra, V. Jain, A. Agarwal, S.K. Guchhait, C.N. Kundu, U.C. Banerjee, P.V. Bharatam, N-fused imidazoles as novel anticancer agents that inhibit catalytic activity of topoisomerase II $\alpha$  and induce apoptosis in G1/S phase, *Journal of Medicinal Chemistry* 54 (2011) 5013–5030.
- [37] K.E. Joung, K.N. Min, D.K. Kim, Y.Y. Sheen, Anti-cancer effect of IN-2001 in T47D human breast cancer, *Biomolecules and therapeutics* 20 (2012) 81–88.
- [38] SYBYL-X 1.2, Tripos International, 1699 South Hanley Rd., St. Louis, Missouri, 63144, USA.